

Investigation of third-order optical nonlinearity in $\text{KBe}_2\text{BO}_3\text{F}_2$ crystal by Z-scan

F.-Q. Li · N. Zong · F.-F. Zhang · J. Yang · F. Yang ·
Q.-J. Peng · D.-F. Cui · J.-Y. Zhang · X.-Y. Wang ·
C.-T. Chen · Z.-Y. Xu

Received: 29 October 2011 / Revised version: 11 January 2012 / Published online: 31 March 2012
© Springer-Verlag 2012

Abstract The third-order optical nonlinearity of deep-ultraviolet (DUV) nonlinear optical (NLO) crystal $\text{KBe}_2\text{BO}_3\text{F}_2$ (KBBF) was investigated using single-beam Z-scan technique for the first time. The Z-scans were performed on a c-cut KBBF crystal and a KBBF prism-coupling device (PCD) with picosecond pulses at 355 nm. No two-photon absorption was observed in the experiment. The measured nonlinear refraction index n_2 showed positive signs, indicating self-focusing Kerr effects. The n_2 values were estimated to be $(1.75 \pm 0.35) \times 10^{-15} \text{ cm}^2/\text{W}$ with the c-cut sample and $(1.85 \pm 0.37) \times 10^{-15} \text{ cm}^2/\text{W}$ with the PCD, corresponding to the third-order nonlinear optical susceptibilities $\chi_{\text{eff}}^{(3)}$ of $(0.99 \pm 0.20) \times 10^{-13} \text{ esu}$ and $(0.94 \pm 0.19) \times 10^{-13} \text{ esu}$, respectively. The results are expected to promote the investigation of frequency conversion processes with ultra-short laser in KBBF crystal.

1 Introduction

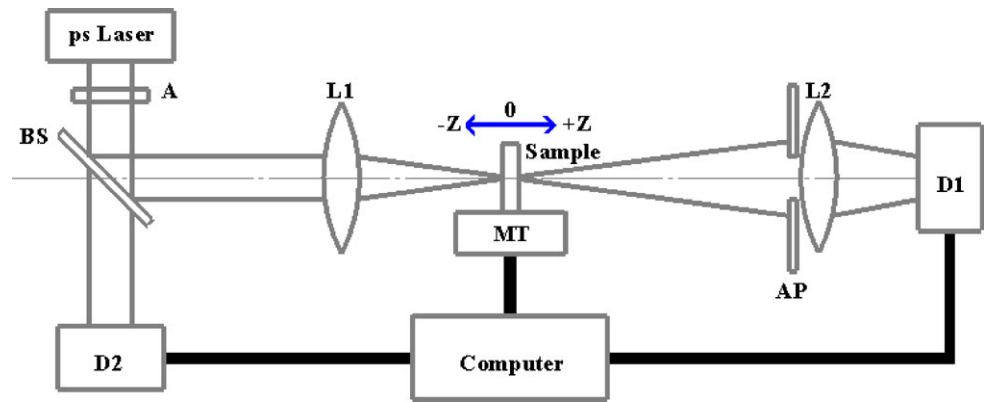
The laser sources in the deep-ultraviolet (DUV) region are very useful in the fields of semiconductor lithography, laser micromachining, photoemission spectroscopy, Raman spectrometer, and so on. Nonlinear optical crystal $\text{KBe}_2\text{BO}_3\text{F}_2$ (KBBF) has high spectral transmission in the UV-DUV region with cut-off wavelength at 150 nm, and it is currently the most important crystal that is capable of producing DUV coherent light through second-harmonic generation (SHG) [1–3]. Due to the strong layer tendency along the optical axis of KBBF and the difficulties in growing, it is hard to cut this crystal along the phase-matching direction. To solve this problem, a special prism-coupling device (PCD) is developed, and the unique KBBF-PCD allows to achieve phase matching for frequency doubling into the DUV regime with a thin KBBF [4, 5]. Based on the KBBF-PCD, both frequency-fixed coherence DUV radiation at 177.3 nm and widely tunable DUV radiation from 170 to 232.5 nm have been generated through direct SHG of third harmonic generation (THG) from Nd:YAG laser at 355 nm and tunable frequency-doubled Ti:sapphire laser from 340 to 465 nm, respectively [6, 7]; and recently, the even shorter wavelength down to 153 nm has been realized by sum-frequency generation (SFG) from Yb-doped laser at 1074 nm and its sixth harmonic beam at 179 nm [8]. The 177.3 nm source has been successfully applied to an angle-resolved photoemission system with a super-high energy resolution better than 1 meV [9]. Except for generating DUV radiation, the KBBF crystal could also be employed for generation of UV radiation [10] and ultra-broadband optical parametric amplification in visible region [11]. To understand the frequency conversion processes in KBBF better, we have recently developed a numerical model for nanosec-

F.-Q. Li · N. Zong · F.-F. Zhang · J. Yang · F. Yang · Q.-J. Peng ·
D.-F. Cui · J.-Y. Zhang · Z.-Y. Xu (✉)
RCLPT, Key Lab of Functional Crystal and Technology,
Technical Institute of Physics and Chemistry, Chinese Academy
of Sciences, Beijing 100190, China
e-mail: zyxu@mail.ipc.ac.cn
Fax: +86-10-82543472

X.-Y. Wang · C.-T. Chen
Beijing Center for crystal R&D, Key Lab of Functional Crystal
and Technology, Technical Institute of Physics and Chemistry,
Chinese Academy of Sciences, Beijing 100190, China

F.-F. Zhang · J. Yang
Graduate School of the Chinese Academy of Sciences, Beijing
100190, China

Fig. 1 Schematic diagram of experimental Z-scan set-up. ps Laser: frequency-tripled Nd:YAG picosecond laser at 355 nm; A Attenuator; BS 50/50 Beam Splitter; L1, L2 Lenses; MT Motor Track; D1, D2 Detectors; AP Aperture



ond KBBF-SHG [4]. While for pico or femtosecond ultrashort pulses with high peak power, the third-order nonlinearity may introduce self-phase modulation (SPM) and cross-phase modulation (XPM), which results in nonlinear phase mismatching and reduces the optical conversion efficiency during the frequency conversion process, it could also result in beam self-focusing or self-defocussing, pulse broadening or compression, and distortion on temporal and spectral profile of the pulse [12–15]. In addition, our recent experiments show that there is considerable pulse-broadening in the generated femtosecond DUV radiation via SHG in KBBF. Therefore, the investigation on the third-order optical nonlinearity of KBBF is expected to be of great importance.

Many techniques have been developed to measure the third-order nonlinear coefficients, such as nonlinear interferometry [16], four-wave mixing [17], nonlinear ellipse rotation (NER) [18], and Z-scan [19]. The Z-scan technique is often used because of its simplicity, sensitivity, accuracy, and the ease of separation between nonlinear absorption and nonlinear refraction.

In this paper, we report the first investigation on the third-order optical nonlinearity of KBBF using single-beam Z-scan technique. Both a c-cut KBBF plate and a KBBF PCD were used for third-order nonlinear investigation with picosecond laser pulses at 355 nm. No two-photon absorption was observed, and the signs of the nonlinear refraction index n_2 were found to be positive, indicating self-focusing Kerr effects in KBBF crystal. The n_2 values were estimated to be $(1.75 \pm 0.35) \times 10^{-15} \text{ cm}^2/\text{W}$ with the c-cut sample and $(1.85 \pm 0.37) \times 10^{-15} \text{ cm}^2/\text{W}$ with the PCD, and the corresponding effective third-order nonlinear optical susceptibilities $\chi_{\text{eff}}^{(3)}$ were calculated to be $(0.99 \pm 0.20) \times 10^{-13} \text{ esu}$ and $(0.94 \pm 0.19) \times 10^{-13} \text{ esu}$, respectively. Our work would provide important information for the investigation on nonlinear optical frequency conversion processes of ultrashort pulses in KBBF.

2 Experiment

The Z-scan technique is based on self-focusing or self-defocusing of the laser beam in a thin nonlinear medium with the sample thickness L shorter than the Rayleigh length z_0 of the laser beam. The nonlinear two-photon absorption of the medium could be estimated by performing an open-aperture Z-scan experiment, while the nonlinear refraction can be extracted from a closed-aperture one. Figure 1 shows the schematic diagram of our experiment, in which an autocontrol and processing system was adopted. The laser source was a frequency-tripled picosecond mode-locked Nd:YAG laser emitting linearly polarized TEM₀₀ pulses having Gaussian-shaped beam profile both spatially and temporally at 355 nm (PL2143B, EKSPLA) with a repetition rate of 10 Hz. The pulse duration for the fundamental wave at 1064 nm was 25 ps, and the pulse width was estimated to be about 15 ps at 355 nm. The light passed through a neutral attenuator (A) and then was approximately equally split into two beams by a beam splitter (BS). One beam was used as the reference to monitor the fluctuation of the laser energy, and the other was used as the pump which was focused onto the sample by a lens L1. The focal length of the lens was about 30 cm, and the focused spot radius w_0 in air at the focal point was about 17.1 μm , corresponding to a Rayleigh length z_0 of about 2.6 mm. The sample was mounted on a motor track (MT), which was controlled by a computer. As the sample moving along near the focal point, the intensity of the pump exiting from the sample changed and so did the transmitted light after a far-field aperture (AP). The transmitted pump light through the aperture was collected by a second lens L2, and the transmitted pump light and the reference signal were recorded simultaneously by two synchronized detectors of D1 and D2 from a dual-channel energy meter (EPM2000). The data from the two detectors were averaged over ten laser shots and then processed by the computer. When the aperture was removed, open-aperture Z-scans were performed.

Two samples, a c-cut KBBF plate and a KBBF PCD for frequency doubling of 355 nm radiation, were adopted to

investigate the third-order optical nonlinearities in KBBF. The c -cut KBBF plate was uncoated with dimensions of 6 (the a -axis) $\times 14 \times 1.09 \text{ mm}^3$, where 1.09 mm is the thickness along its optical axis (c -axis). For the KBBF PCD, the KBBF crystal with the dimensions of 6 (the a -axis) $\times 14 \times 0.75 \text{ mm}^3$ (the optical c -axis) was sandwiched between two CaF_2 prisms through optical contact, and this caused enlargement of the beam waist w_0 to $\sqrt{n_c}w_0$ with $n_c = 1.447$ being the refractive index of CaF_2 at 355 nm , therefore the Rayleigh length was $n_c z_0$ in the CaF_2 KBBF PCD case; The surfaces of both KBBF and the CaF_2 prisms were also uncoated; The phase-matching condition is satisfied if the 355 nm laser propagates along the phase-matching angle with the light polarization parallel to the a -axis, which is illustrated in Fig. 2.

When performing Z-scan measurements on the c -cut KBBF, the light propagated along the optical axis of the crystal, and the light polarization was along the a -axis. While during Z-scans with the CaF_2 -KBBF PCD, the laser impinged on the front face of CaF_2 prism perpendicularly, resulting in an actual KBBF crystal thickness of $L = 0.75 \text{ mm} / \cos(\theta)$, with θ being the refractive angle in KBBF at the CaF_2 -KBBF interface. It should be pointed out that the CaF_2 -KBBF PCD was for frequency doubling of 355 nm radiation with light polarization parallel to the a -axis ($E \parallel a$ -axis), and the second-order nonlinear optical susceptibility may manifest itself in the Z-scans through the cascaded

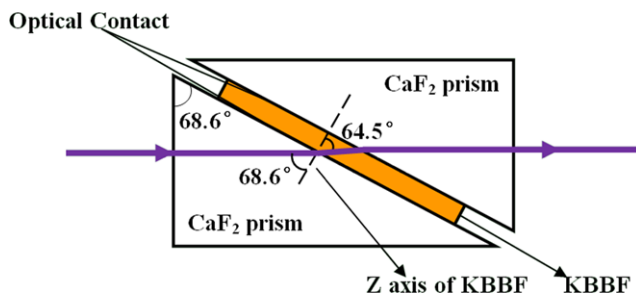
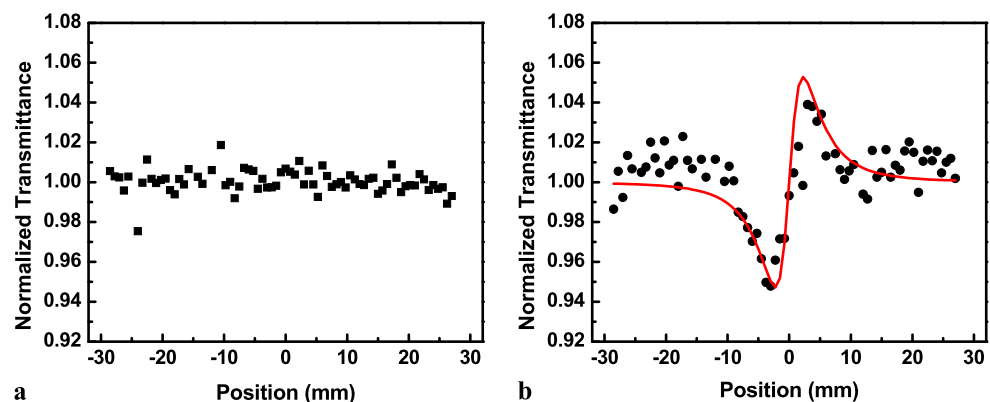


Fig. 2 Structure of the optically contacted KBBF- CaF_2 prism-coupled device (PCD)

Fig. 3 Z-scan results with c -cut KBBF: (a) Open-aperture Z-scans, indicating no nonlinear two-photon absorption; and (b) closed-aperture Z-scans



effect [20]. Therefore, we performed the Z-scans with the polarization perpendicular to the a -axis ($E \perp a$ -axis) with the PCD sample to avoid phase matching and second harmonic generation.

In our experiment, the experimental error mainly originated from the determination of the beam waist, the pulse width and the pulse energy entered the KBBF crystal. The compound error was estimated to be about 20 %.

3 Results and discussions

The open-aperture Z-scan results with the c -cut KBBF and the KBBF PCD are shown in Fig. 3(a) and Fig. 4(a), respectively. It can be seen that both signals of the open-aperture Z-scans were nearly flat, which indicates that nonlinear two-photon absorption is negligible in our experiment. This is anticipated because two-photon energy of the laser wavelength at 355 nm is below the band-gap energy of KBBF [21–23].

The closed-aperture Z-scans are sensitive to both the nonlinear absorption and nonlinear refraction. With small or ignorable nonlinear absorption in closed-aperture Z-scan experiment, the light transmittance T through the far-field aperture is described by [19]

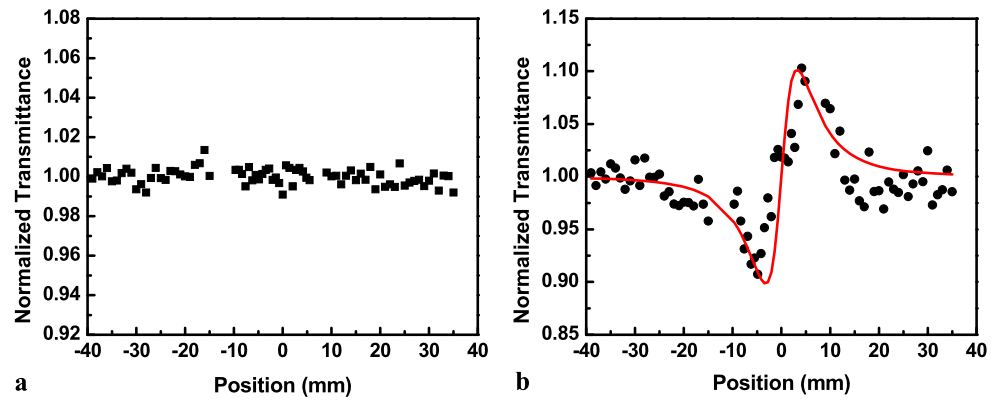
$$T(x, \langle \Delta \Phi_0 \rangle) \approx 1 + \frac{4 \langle \Delta \Phi_0 \rangle x}{(x^2 + 9)(x^2 + 1)}, \quad (1)$$

where $\langle \Delta \Phi_0 \rangle$ is the time averaged phase shift and $x = z/z_0$ is the translation coordinate normalized by the Rayleigh length of the focused beam $z_0 = kw_0^2/2$ with k being the wave-vector. The time averaged phase shift $\langle \Delta \Phi_0 \rangle$ can be determined by fitting the experimental data using Eq. (1). Usually, $\langle \Delta \Phi_0 \rangle$ could be calculated directly from the relation [19]

$$\Delta T_{pv} \approx 0.406(1 - S_a)^{0.25} |\langle \Delta \Phi_0 \rangle|, \quad \text{for } |\langle \Delta \Phi_0 \rangle| \leq \pi \quad (2)$$

where ΔT_{pv} is the difference between the peak and valley of the transmittance, and $S_a = 1 - \exp(-2r_a^2/w_a^2)$ is the linear

Fig. 4 Z-scan results with KBBF PCD: (a) Open-aperture Z-scans, indicating no nonlinear two-photon absorption; and (b) closed-aperture Z-scans



transmittance of the far-field aperture with r_a being the radius of the aperture and w_a the radius of the laser beam on the aperture. During our experiment, the aperture transmittance S_a was actually calculated after measuring the transmitted pulse energies with and without the aperture, respectively, when the sample was kept far away from the focal point. Assuming a Gaussian temporal shape beam, the averaged phase shift $\langle \Delta \Phi_0 \rangle$ is related to the peak on-axis phase shift $\Delta \Phi_0$ by $\langle \Delta \Phi_0 \rangle = \Delta \Phi_0 / \sqrt{2}$. Thus, the nonlinear refractive index n_2 is calculated from [24]

$$n_2 \approx \frac{0.38 w_0^2 \tau \lambda}{E_p L_{\text{eff}}} \langle \Delta \Phi_0 \rangle, \quad (3)$$

where λ is the laser wavelength, τ_p is the FWHM pulse width, E_p is the pulse energy entering into the sample under study, and $L_{\text{eff}} = (1 - \exp(-\alpha L)) / \alpha$ is the effective sample length with α being the linear absorption coefficient and L being the actual thickness of the sample along the optical path. The linear absorption coefficient for KBBF was about 0.13 cm^{-1} at 355 nm [4].

To determine the pulse energy entered the samples as accurately as possible, we measured the energy ratio of the incident laser on the samples to the reference beam before the Z-scan measurements, and then the incident pulse energy on the samples could be calculated by multiplying this ratio with the average pulse energy of the reference beam recorded through the Z-scans. For the c-cut KBBF crystal, the Fresnel reflection loss at the front face was taken into account to further calculate the pulse energy entered the sample exactly. As for the CaF_2 -KBBF PCD, there were energy losses caused by the Fresnel reflection at the air- CaF_2 and CaF_2 -KBBF interfaces as well as linear absorption introduced by CaF_2 prism in front of the KBBF crystal. The Fresnel reflection loss at the air- CaF_2 interface could be calculated from the linear refraction index of CaF_2 , and the linear absorption of the CaF_2 prism could be estimated from the linear absorption coefficients of the CaF_2 crystal and the light propagation depth in it. Because the linear refractive index of CaF_2 is close to that of KBBF, we ignored the Fresnel reflection loss at the CaF_2 -KBBF interfaces. Thus, with

the CaF_2 -KBBF PCD, the accurate pulse energy entered the KBBF crystal could be corrected by further subtracting the losses mentioned above. It is worth mentioning here that the laser pulse energy has to be selected carefully during our Z-scan measurements, because at low pulse energy, there would be relatively large fluctuations with the Z-scan curves due to the low signal-to-noise ratio, while at high pulse energy, damage could occur to the KBBF sample. Thus, we performed every Z-scan measurement at a moderate pulse energy, and the results can be as trustful as that with the measurements performed at several different pulse energies [19, 25].

Figures 3(b) and 4(b) show the closed-aperture Z-scan results for the c-cut KBBF plate and the KBBF PCD, respectively, where the dots are experimental data and the solid lines are fitting curves with Eq. (1). It can be seen that the closed-aperture Z-scan traces show valley-peak variations, indicating positive signs of the nonlinear refractive index n_2 and self-focusing Kerr effects in KBBF.

For the c-cut sample, the linear transmittance S_a during the experiment was measured to be about 0.24. The pulse energy entering into the crystal was $\sim 0.80 \mu\text{J}$ after taking into account the surface Fresnel loss. The nonlinear refraction index n_2 were then determined to be $(1.75 \pm 0.35) \times 10^{-15} \text{ cm}^2/\text{W}$.

For the CaF_2 -KBBF PCD, the linear transmittance S_a was measured to be about 0.18, and the pulse energy entered the crystal was $\sim 0.97 \mu\text{J}$ after taking into account the losses caused by the linear absorption of CaF_2 and the surface Fresnel reflections. To take into account the influence of the CaF_2 prisms on the third-order nonlinear measurements, we also performed Z-scans on a $\Phi 20 \text{ mm} \times 2 \text{ mm}$ CaF_2 crystal under the same condition, and no nonlinear response was observed with CaF_2 crystal. Therefore, we concluded that the third-order nonlinearity observed in the KBBF-PCD could be solely attributed to the contribution by the KBBF crystal. Taking into account the influence of CaF_2 on the beam waist and on the translation coordinates, the nonlinear refraction index n_2 were estimated to be $(1.85 \pm 0.37) \times 10^{-15} \text{ cm}^2/\text{W}$.

Table 1 Measured nonlinear refractive index n_2 , susceptibility $\chi_{\text{eff}}^{(3)}$ of KBBF crystal at 355 nm

Sample	n_0 [26]	S_a	E_p (μJ)	n_2 (10^{-16} cm ² /W)	$\chi_{\text{eff}}^{(3)}$ (10^{-13} esu)
c-cut KBBF	1.497	0.24	0.80	1.75 (± 0.35)	0.99 (± 0.2)
KBBF PCD	1.419	0.18	0.97	1.85 (± 0.37)	0.94 (± 0.19)

We then calculated the effective third-order nonlinear optical susceptibility $\chi_{\text{eff}}^{(3)}$ according to [25]

$$\text{Re}[\chi_{\text{eff}}^{(3)}(\text{esu})] = 10^{-4} \frac{\varepsilon_0 c^2 n_0^2}{\pi} n_2 \left(\frac{\text{cm}^2}{\text{W}} \right), \quad (4)$$

where ε_0 is the vacuum permittivity, c is the light velocity in vacuum, and n_0 is the linear refractive index. The third-order susceptibilities were calculated to be $(0.99 \pm 0.20) \times 10^{-13}$ esu for the c-cut sample and $(0.94 \pm 0.19) \times 10^{-13}$ esu for the KBBF PCD sample, respectively. It can be seen that, the third-order nonlinear susceptibilities are nearly same in the two different KBBF samples. The results and the parameters used for the calculations are summarized in Table 1.

4 Conclusion

The third-order nonlinearity of nonlinear optical crystal KBBF was investigated with two KBBF samples using the Z-scan technique by picosecond laser at 355 nm. No nonlinear absorption was observed. The experimental results show that the nonlinear refraction and third-order susceptibility in the two samples coincide well with each other. The nonlinear refractive index n_2 was around 1.8×10^{-15} cm²/W with a positive sign indicating a self-focusing effect in the KBBF. The effective third-order nonlinear optical susceptibility $\chi_{\text{eff}}^{(3)}$ was about 1.0×10^{-13} esu. Our work provides useful information for this unique DUV crystal and hopefully could promote the investigation of dynamics processes of nonlinear optical frequency conversion for the ultrashort pulses in the KBBF.

Acknowledgements This work is supported by the State Key Program for Basic Research of China (Grant No. 2010CB630760), the National High Technology Research and Development Program, the National Natural Science Foundation of China, and the Knowledge Innovation Program of Chinese Academy of Sciences. The authors gratefully acknowledge Dong-Xiang Zhang and Ting-Yin Ning for their discussion and technical assistance in the experiment, and acknowledge Bao-Hua Feng for his great support on our work.

References

1. C. Chen, Z. Xu, D. Deng, J. Zhang, G.K.L. Wong, B. Wu, N. Ye, D. Tng, Appl. Phys. Lett. **68**, 2930 (1996)
2. C.T. Chen, T. Kanai, X.Y. Wang, Y. Zhu, S. Watanabe, Opt. Lett. **33**, 282 (2008)
3. Y. Zhang, Y. Sato, N. Watanabe, R. Ananda, Y. Okada-Shudo, M. Watanabe, M. Hyodo, X.Y. Wang, C. Chen, T. Kanai, S. Watanabe, Opt. Express **17**, 8119 (2009)
4. F. Yang, Z. Wang, Y. Zhou, F. Li, J. Xu, Y. Xu, X. Cheng, Y. Lu, Y. Bo, Q. Peng, D. Cui, X. Zhang, X. Wang, Y. Zhu, Z. Xu, Appl. Phys. B **96**, 415 (2009)
5. C. Chen, Opt. Mater. **26**, 425 (2004)
6. G. Wang, X. Wang, Y. Zhou, Y. Chen, C. Li, Y. Zhu, Z. Xu, C. Chen, Appl. Phys. B **91**, 95 (2008)
7. X. Zhang, Z. Wang, G. Wang, Y. Zhu, Z. Xu, C. Chen, Opt. Lett. **34**, 1342 (2009)
8. Y. Nomura, Y. Ito, A. Ozawa, X.Y. Wang, C.T. Chen, S. Shin, S. Watanabe, Y. Kobayashi, Opt. Lett. **36**, 1758 (2011)
9. W. Zhang, G. Liu, L. Zhao, H. Liu, J. Meng, X. Dong, W. Lu, J.S. Wen, Z.J. Xu, G.D. Gu, T. Sasagawa, G. Wang, Y. Zhu, H. Zhang, Y. Zhou, X. Wang, Z. Zhao, C. Chen, Z. Xu, X.J. Zhou, Phys. Rev. Lett. **100**, 107002 (2008)
10. J.H. Lu, G.L. Wang, Z.Y. Xu, C.T. Chen, J.Y. Yang, C.Q. Zhang, Y.G. Liu, Opt. Commun. **200**, 415 (2001)
11. P. Kumbhakar, T. Kobayashi, Opt. Commun. **277**, 205 (2007)
12. T. Ditmire, A.M. Rubenchik, D. Eimerl, M.D. Perry, J. Opt. Soc. Am. B **13**, 649 (1996)
13. I.A. Begishev, M. Kalashnikov, V. Karpov, P. Nickles, H. Schönengel, I.A. Kulagin, T. Usmanov, J. Opt. Soc. Am. B **21**, 318 (2004)
14. D. Pang, R. Zhang, Q. Wang, Opt. Commun. **196**, 293 (2001)
15. J.Y. Zhang, J.Y. Huang, H. Wang, K.S. Wong, G.K. Wong, J. Opt. Soc. Am. B **15**, 200 (1998)
16. M.J. Moran, C.Y. She, R.L. Carman, IEEE J. Quantum Electron. **QE-11**, 259 (1975)
17. S.R. Friberg, P.W. Smith, IEEE J. Quantum Electron. **QE-23**, 2089 (1987)
18. A. Owyong, IEEE J. Quantum Electron. **QE-9**, 1064 (1973)
19. M. Sheik-Bahae, A.A. Said, T.H. Wei, D.J. Hagan, E.W. Van Stryland, IEEE J. Quantum Electron. **26**, 760 (1990)
20. R. DeSalvo, D.J. Hagan, M. Sheik-Bahae, G. Stegeman, E.W. Van Stryland, H. Vanherzeele, Opt. Lett. **17**, 28 (1992)
21. M. Sheik-Bahae, D.C. Hutchings, D.J. Hagan, E.W. VanStryland, IEEE J. Quantum Electron. **27**, 1296 (1991)
22. R. DeSalvo, A.A. Said, D.J. Hagan, E.W. Van Stryland, M. Sheik-Bahae, IEEE J. Quantum Electron. **32**, 1324 (1996)
23. H. Li, F. Zhou, X. Zhang, W. Ji, Opt. Commun. **144**, 75 (1997)
24. S. Miller, F. Rotermund, G. Xu, F. Noack, V. Panyutin, V. Petrov, Opt. Mater. **30**, 1469 (2008)
25. T. Geethakrishnan, P.K. Palanisamy, Opt. Commun. **270**, 424 (2007)
26. C. Chen, G. Wang, X. Wang, Y. Zhu, Z. Xu, T. Kanai, S. Watanabe, IEEE J. Quantum Electron. **44**, 617 (2008)